

# Detection of Protein Biomarkers Using RNA Aptamer Microarrays and Enzymatically Amplified Surface Plasmon Resonance Imaging

Yuan Li, Hye Jin Lee, and Robert M. Corn\*

Department of Chemistry, University of California—Irvine, Irvine, California 92697

A methodology for the detection of protein biomarkers at picomolar concentrations that utilizes surface plasmon resonance imaging (SPRI) measurements of RNA aptamer microarrays is developed. The adsorption of proteins onto the RNA microarray is detected by the formation of a surface aptamer–protein–antibody complex. The SPRI response signal is then amplified using a localized precipitation reaction catalyzed by the enzyme horseradish peroxidase that is conjugated to the antibody. This enzymatically amplified SPRI methodology is first characterized by the detection of human thrombin at a concentration of 500 fM; the appropriate thrombin aptamer for the sandwich assay is identified from a microarray of three potential thrombin aptamer candidates. The SPRI method is then used to detect the protein vascular endothelial growth factor (VEGF) at a biologically relevant concentration of 1 pM. VEGF is a signaling protein that has been used as a serum biomarker for rheumatoid arthritis, breast cancer, lung cancer, and colorectal cancer and is also associated with age-related macular degeneration.

The rapid detection and profiling of multiple protein biomarkers in blood and serum samples are a potentially powerful method for the diagnosis of diseases and the monitoring of subsequent therapeutic treatments.<sup>1,2</sup> For example, antibody arrays that can detect up to 120 serum biomarkers for the early-stage detection and diagnosis of various cancers are currently available commercially from Whatman Inc. These antibody assays typically use a second set of fluorescently tagged antibodies for the detection of biomarker adsorption to the array elements.<sup>3,4</sup>

Microarrays of RNA aptamers are emerging as an attractive alternative to antibody arrays for the multiplexed bioaffinity detection and identification of protein biomarkers.<sup>5–8</sup> Compared

to antibodies, nucleic acid aptamers are less susceptible to irreversible denaturation, are more amenable to chemical modification, and can be identified by in vitro (as compared to in vivo for antibodies) selection methods.<sup>9–12</sup> Surface RNA aptamer structures can also be reversibly deactivated by the hybridization adsorption of a complementary DNA sequence and can be regenerated by the subsequent desorption of DNA from the aptamer array element.

Surface plasmon resonance imaging (SPRI) has been established as one of the primary optical methods for the direct detection of bioaffinity adsorption onto DNA, protein, and RNA microarrays.<sup>13–18</sup> We have recently employed SPRI for the detection of protein adsorption onto RNA aptamer microarrays down to a concentration of 10 nM.<sup>19</sup> A detection limit of 10 nM is sufficient for the analysis of some biomarkers (e.g.,  $\beta_2$ -microglobulin and cystatin C);<sup>20</sup> however, many important protein biomarkers are present in biological samples at much lower concentrations. For example, the signaling protein vascular endothelial growth factor (VEGF) exists in serum samples at picomolar concentrations and has been identified as a potential biomarker for rheumatoid arthritis and various cancers.<sup>21–24</sup>

\* To whom correspondence should be addressed. E-mail: rcorn@uci.edu.

- (1) de Seny, D.; Fillet, M.; Meuwis, M.-A.; Geurts, P. L.; Laurence, R. C.; Bours, V.; Wehenkel, L.; Piette, J.; Malaise, M.; Merville, M.-P. *Arthritis Rheum.* **2006**, *52*, 3801–3812.
- (2) Poon, T. C.; Sung, J. J. Y.; Chow, S. M.; Ng, E. K. W.; Yu, A. C. W.; Chu, E. S. H.; Hui, A. M. Y.; Leung, W. K. *Gastroenterology* **2006**, *130*, 1858–1864.
- (3) Sapsford, K. E.; Charles, P. T.; Patterson, C. H. J.; Ligler, F. S. *Anal. Chem.* **2002**, *74*, 1061–1068.
- (4) Silzel, J. W.; Cercek, B.; Dodson, C.; Tsay, T.; Obremski, R. J. *Clin. Chem.* **1998**, *44*, 2036–2043.
- (5) Collett, J. R.; Cho, E. J.; Lee, J. F.; Levy, M.; Hood, A. J.; Wan, C.; Ellington, A. D. *Anal. Biochem.* **2005**, *338*, 113–123.
- (6) Stadtherr, K.; Wolf, H.; Lindner, P. *Anal. Chem.* **2005**, *77*, 3437–3443.

- (7) Bock, C.; Coleman, M.; Collins, B.; Davis, J.; Foulds, G.; Gold, L.; Greef, C.; Heil, J.; Hellig, J. S.; Hicke, B.; Hurst, M. N.; Miller, D.; Ostroff, R.; Petach, H.; Schneider, D.; Vant-Hull, B.; Waugh, S.; Weiss, A.; Wilcox, S. K.; Zichi, D. *Proteomics* **2004**, *4*, 609–618.
- (8) McCauley, T. G.; Hamaguchi, N.; Stanton, M. *Anal. Biochem.* **2003**, *319*, 244–250.
- (9) Bunka, D. H. J.; Stockley, P. G. *Nat. Rev. Microbiol.* **2006**, *4*, 588–596.
- (10) Brody, E. N.; Gold, L. *Rev. Mol. Biotechnol.* **2000**, *74*, 5–13.
- (11) Nimjee, S. M.; Rusconi, C. P.; Sullenger, B. A. *Annu. Rev. Med.* **2005**, *56*, 555–583.
- (12) Jayasena, S. *Clin. Chem.* **1999**, *45*, 1628–1650.
- (13) Phillips, K. S.; Wilkop, T.; Wu, J.-J.; Al-Kaysi, R. O.; Cheng, Q. *J. Am. Chem. Soc.* **2006**, *128*, 9590–9591.
- (14) Wolf, L. K.; Fullenkamp, D. E.; Georgiadis, R. M. *J. Am. Chem. Soc.* **2005**, *127*, 17453–17459.
- (15) Shumaker-Parry, J. S.; Campbell, C. T. *Anal. Chem.* **2004**, *76*, 907–917.
- (16) Kanda, V.; Kariuki, J. K.; Harrison, D. J.; McDermott, M. T. *Anal. Chem.* **2004**, *76*, 7257–7262.
- (17) Nelson, B. P.; Grimsrud, T. E.; Liles, M. R.; Goodman, R. M.; Corn, R. M. *Anal. Chem.* **2001**, *73*, 1–7.
- (18) Goodrich, T. T.; Lee, H. J.; Corn, R. M. *Anal. Chem.* **2004**, *76*, 6173–6178.
- (19) Li, Y.; Lee, H. J.; Corn, R. M. *Nucleic Acids Res.* In press.
- (20) Lee, H. J.; Nedelkov, D.; Corn, R. M. *Anal. Chem.* **2006**, *78*, 6504–6510.
- (21) Kuramochi, H.; Hayashi, K.; Uchida, K.; Miyakura, S.; Shimizu, D.; Vallbohmer, D.; Park, S.; Danenberg, K. D.; Takasaki, K.; Danenberg, P. V. *Clin. Cancer Res.* **2006**, *12*, 29–33.
- (22) Raben, D.; Ryan, A. *Clin. Lung Cancer* **2005**, *7*, 175–179.
- (23) Nakahara, H.; Song, J.; Sugimoto, M.; Hagihara, K.; Kishimoto, T.; Yoshizaki, K.; Nishimoto, N. *Arthritis Rheum.* **2003**, *48*, 1521–1529.

For the detection of biomarkers at subpicomolar concentrations in biological samples, enzymatic amplification of the biosensor response is often required. For example, ELISA microwell or membrane assays that use horseradish peroxidase (HRP)-conjugated antibodies with either a fluorogenic or chemiluminescent substrate can be used in solution to detect proteins down to femtomolar concentrations.<sup>25,26</sup> These solution-based fluorescence methods have limited spatial resolution and therefore cannot be used in a surface microarray format. In contrast, an HRP substrate such as 3,3',5,5'-tetramethylbenzidine (TMB) that creates a localized surface precipitation reaction can be used in surface biosensor microarrays with high spatial resolution. This localized precipitation reaction can be detected with either optical or electrochemical methods.<sup>27,28</sup>

In this paper, we show that HRP-conjugated antibodies can be used with SPRI measurements of RNA aptamer microarrays to detect protein biomarkers down to subpicomolar concentrations with a localized precipitation reaction. An RNA aptamer/protein biomarker/antibody–HRP sandwich structure is formed on the microarray surface, and a subsequent localized HRP–TMB precipitation reaction is used to amplify the SPRI response due to specific protein biomarker adsorption onto the RNA aptamer array. The SPRI measurements have a subpicomolar sensitivity; as a first example, human thrombin protein was detected at a concentration of 500 fM using an RNA aptamer identified from a microarray of three potential thrombin aptamer candidates. The protein detection sensitivity of SPRI was improved by a factor of 10 000 through the use of the HRP–TMB precipitation reaction. This amplified method was then used with a second RNA aptamer array to detect the protein biomarker VEGF at a biologically relevant concentration of 1 pM.

## EXPERIMENTAL CONSIDERATIONS

**Materials.** 11-Amino-1-undecanethiol hydrochloride (MUAM; Dojindo), sulfosuccinimidyl 4-(*N*-maleimidomethyl)cyclohexane-1-carboxylate (SSMCC; Pierce), 9-fluorenylmethoxycarbonyl-*N*-hydroxysuccinimide (Fmoc-NHS; Novabiochem), and *N*-hydroxysuccinimidyl ester of methoxypoly(ethylene glycol) propionic acid (MW 2000) (PEG-NHS; Nektar Therapeutics) were all used as received. All unmodified RNA sequences (PAGE purified) were purchased from Dharmacon Research Inc. The DNA anchor probe with 3'-thiol modification and 5'-phosphorylation and the thrombin DNA aptamer D<sub>1</sub> with 3'-thiol modification were purchased from Integrated DNA Technologies and were deprotected and purified using reversed-phase binary elution HPLC. All RNA and DNA sequences are listed in Table 1. Human thrombin (Haematologic Technologies Inc.), unmodified thrombin antibody, HRP-conjugated thrombin antibody (Enzyme Research), recombinant human VEGF (165-amino acid residues; Sigma-Aldrich), biotinylated anti-

**Table 1. Summary of All DNA and RNA Sequences Used for the Enzymatically Amplified SPRI Detection of hTh and VEGF<sup>a</sup>**

DNA anchor probe:	5'-PO <sub>4</sub> <sup>2-</sup> -TT(A) <sub>18</sub> (CH <sub>2</sub> ) <sub>6</sub> -S-S-3'
thrombin DNA aptamer (D <sub>1</sub> ):	5'-AGT CCG TGG TAG GGC AGG TTG GGG TGA CT-(T) <sub>15</sub> (CH <sub>2</sub> ) <sub>6</sub> -S-S-3'
thrombin RNA aptamer 1 (R <sub>1</sub> ):	5'-GGG AAC AAA GCU GAA GUA CUU ACC C (A) <sub>8</sub> -3'
thrombin RNA aptamer 2 (R <sub>2</sub> ):	5'-UUU GGA AGA UAG CUG GAG AAC UAA CCA AA (A) <sub>8</sub> -3'
VEGF RNA aptamer (R <sub>V</sub> ):	5'-CCG GUA GUC GCA UGG CCC AUC GCG CCC GG (A) <sub>8</sub> -3'
control RNA aptamer (R <sub>C</sub> ):	5'-AGA CUC UGA CUC AGU G-3'

<sup>a</sup> Fifteen thymine bases were attached to the 3'-end of the D<sub>1</sub> aptamer as a spacer to place the aptamer further away from the surface. Eight adenosine bases were added to the 3'-ends of RNA aptamers R<sub>1</sub>, R<sub>2</sub>, and R<sub>V</sub> to facilitate the surface ligation reaction.

VEGF antibody (R&D Systems), anti-biotin HRP (Jackson Immuno-Research), and T4 RNA ligase (Epicentre Biotechnology) were all diluted to the desired concentration before use. HEPES buffer (20 mM HEPES, 150 mM NaCl, 2 mM CaCl<sub>2</sub>, pH 7.4) was used for all thrombin measurements. PBS buffer (10.0 mM Na<sub>2</sub>HPO<sub>4</sub>, 137 mM NaCl, 2.7 mM KCl, pH 7.4) was used for all VEGF measurements. The stock solution of TMB substrate (BioFX Laboratories; TMB one-component small particle membrane substrate, proprietary concentration) was diluted 10 times in either HEPES buffer (thrombin detection) or PBS buffer (VEGF detection) for the surface precipitation reactions. All buffers and water were autoclaved prior to use.

**DNA Microarray Fabrication.** DNA microarrays were fabricated using a seven-step chemical modification process described previously.<sup>29</sup> Thin gold films (45 nm) were deposited onto SF-10 glasses (Schott Glass) using a Denton DV-502A metal evaporator with a 1-nm underlayer of chromium. The gold surfaces were first modified with a self-assembled monolayer of the amine-terminated alkanethiol MUAM. This MUAM surface was then reacted with Fmoc-NHS to form a hydrophobic background. Next, the Fmoc surface was exposed to UV light with a quartz mask containing 500-μm square features to create bare gold spots within the hydrophobic Fmoc background. The bare gold spots were then reacted with MUAM for 2 h followed by the SSMCC reaction. The SSMCC solution was manually spotted using a picopump onto the MUAM array elements to form a thiol-reactive, maleimide-terminated surface. Thiol-modified DNA sequences were then spotted onto the individual SSMCC array elements and allowed to react overnight. Upon completion of the DNA attachment reaction, the DNA array was thoroughly rinsed with sterile Millipore water, dried in a nitrogen stream, and used immediately for the creation of RNA microarrays via surface RNA–DNA ligation reactions.

**Aptamer Microarray Fabrication.** RNA aptamer microarrays were fabricated using a surface RNA–DNA ligation methodology catalyzed by the enzyme T4 RNA ligase as described previously.<sup>19</sup> In brief, a DNA anchor probe with 3'-thiol and 5'-phosphate

(24) Adams, J.; Carder, P. J.; Downey, S.; Forbes, M. A.; MacLennan, K.; Allgar, V.; Kaufman, S.; Hallam, S.; Bicknell, R.; Walker, J. J.; Cairnduff, F.; Selby, P. J.; Perren, T. J.; Landsdown, M.; Banks, R. *Cancer Res.* **2000**, *60*, 2898–2905.

(25) Roda, A.; Mirasoli, M.; Guardigli, M.; Michelini, E.; Simoni, P.; Magliulo, M. *Anal. Bioanal. Chem.* **2006**, *384*, 1269–1275.

(26) Huang, R.-P. *J. Immunol. Methods* **2001**, *255*, 1–13.

(27) Kim, S. D.; Chung, J. W.; Kim, J. T.; H., K.; Pyun, J. C. *Sens. Actuators, B* **2005**, *111–112*, 463–469.

(28) Zhong, X.-b.; Leng, L.; Beitin, A.; Chen, R.; McDonald, C.; Hsiao, B.; Jenison, R. D.; Kang, I.; Park, S.-H.; Lee, A.; Gregersen, P.; Thuma, P.; Bray-Ward, P.; Ward, D. C.; Bucala, R. *Nucleic Acids Res.* **2005**, *33*, e121.

(29) Brockman, J. M.; Frutos, A. G.; Corn, R. M. *J. Am. Chem. Soc.* **1999**, *121*, 8044–8051.

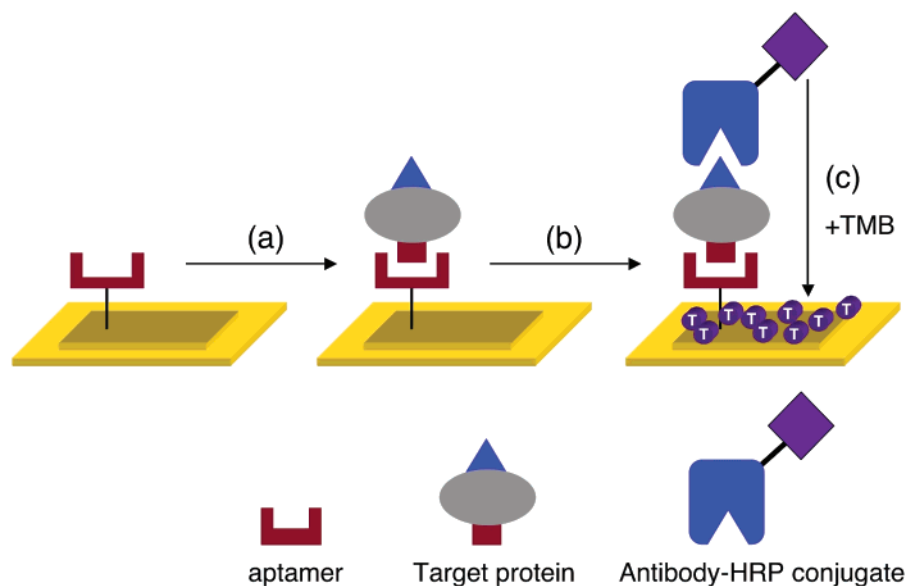


**Figure 1.** Schematic outlining the enzymatically amplified SPRI detection of target proteins. In step a, the target protein binds to the surface-immobilized aptamer. Next, in step b, an HRP-conjugated antibody to the target protein is introduced to create a surface aptamer–protein–antibody sandwich structure. In step c, this surface is exposed to the substrate TMB, which reacts with HRP to form a dark blue precipitate on the array elements containing the aptamer–protein–antibody complex. A very small amount of this precipitate on the gold surface results in a significantly amplified SPRI response.

modifications (see Table 1 for the sequence) was immobilized on a chemically modified gold surface via a surface thiol/maleimide reaction to create a DNA microarray containing identical DNA sequences in each array element. Various unmodified single-stranded RNA (ssRNA) sequences were then ligated to individual DNA array elements using T4 RNA ligase. T4 RNA ligase and ssRNA were mixed in a 40 mM Tris buffer (10 mM  $\text{MnCl}_2$ , 100  $\mu\text{M}$  ATP, and 10 mM DTT, pH 7.5) to have a final concentration of 0.5 unit/ $\mu\text{L}$  and 10  $\mu\text{M}$ , respectively. Approximately 30 nL of this reaction mixture was then manually spotted using a picopump to each 500  $\mu\text{m} \times 500 \mu\text{m}$  DNA array element and allowed to react for 3 h at room temperature. For the case of aptamer microarrays containing DNA aptamer array elements, the 3'-thiol-modified DNA aptamer was immobilized as described in the previous section and no ligation solution was spotted to array elements containing the DNA aptamer. After the ligation reaction was completed, the microarray was thoroughly rinsed with sterile Millipore water to remove the enzyme and any nonligated RNA. Next the microarray was exposed to a mildly basic solution to remove the Fmoc hydrophobic background and to regenerate the amine-terminated MUAM surface. The MUAM surface was then reacted with PEG-NHS to create a background resistant to the nonspecific adsorption of biomolecules. The RNA microarray was finally rinsed with sterile Millipore water, dried in a nitrogen stream, and used for SPRI measurements.

**SPR Imaging Measurements.** An SPR imager (GWC Technologies) using near-infrared excitation from an incoherent white light source was used for the enzymatically amplified detection of thrombin and VEGF proteins. A simplified scheme of the SPR imager setup is shown in Figure S.1 in the Supporting Information. Briefly, the white light beam is passed through a polarizer to generate p-polarized light, which then impinges on a prism/thin gold film assembly at a fixed incident angle slightly smaller than the SPR angle. The reflected light is collected with a CCD camera

after passing through a narrow band-pass filter centered at 830 nm. SPRI data were collected using the software V++ 4.0 (Digital Optics) and further analyzed using NIH Image 1.63.

## RESULTS AND DISCUSSION

Enzymatically amplified SPRI measurements of RNA aptamer microarrays are used to identify and detect proteins at subpicomolar concentrations. Figure 1 illustrates the scheme of the enzymatic reaction for the amplified SPRI detection of proteins. A surface-immobilized aptamer is used to capture the proteins onto the RNA microarray, and then an antibody conjugated with HRP is bound to the array element via the formation of an aptamer–protein–antibody sandwich structure. On the addition of the substrate TMB, HRP catalyzes the localized formation of a dark blue precipitate that is detected using SPRI measurements. This enzymatically amplified SPRI methodology was characterized by the detection of human thrombin (hTh), a 37-kDa serine protease that is commonly used to enhance clot formation in blood samples<sup>30</sup> and then employed for the detection of VEGF, a 42-kDa signaling protein that stimulates new blood vessel formation in cells.<sup>31</sup>

Section A details how SPRI was used to select the best thrombin aptamer for the formation of aptamer–hTh–antibody structures from a number of thrombin aptamer candidates. Section B presents the detection of hTh at subpicomolar concentrations using the enzymatically amplified SPRI methodology. Finally, section C describes a modified sandwich assay that employs a biotinylated VEGF antibody and an anti-biotin-conjugated HRP for the detection of VEGF at picomolar concentrations with SPRI.

**A. SPRI Measurements of Aptamer–Thrombin–Antibody Structures.** Several researchers have independently generated RNA and DNA aptamers that bind to thrombin in an effort to

(30) Jackson, M. R. *Am. J. Surg.* **2001**, *182*, 1S–7S.

(31) Risau, W. *Nature* **1997**, *386*, 671–674.

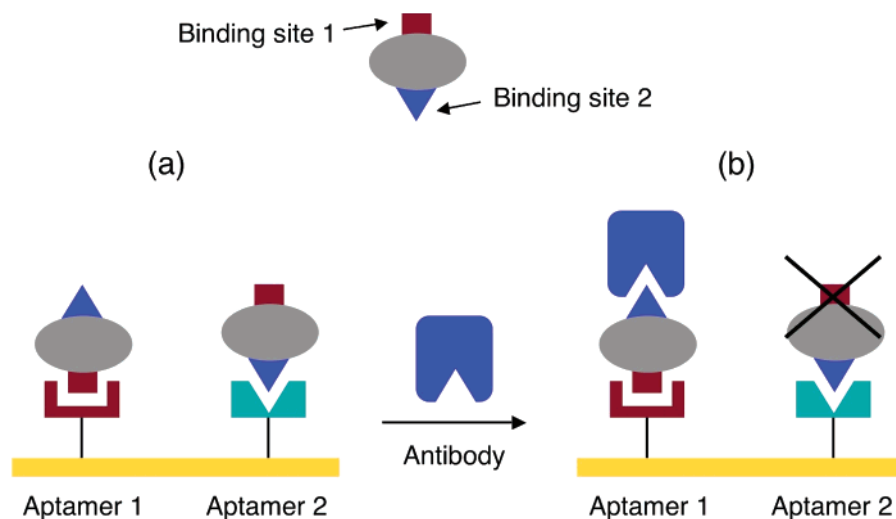


**Figure 2.** Schematic illustration for the formation of a surface aptamer–protein–antibody sandwich structure. (a) Two different aptamers 1 and 2 that bind to the same target protein are attached to the surface. The target protein binds to the two aptamers via different binding sites: aptamer 1 binds to binding site 1 on the protein while aptamer 2 binds to binding site 2 on the protein. (b) When an antibody that binds to binding site 2 on the target protein is introduced, only aptamer 1, but not aptamer 2, will form a surface aptamer–protein–antibody sandwich structure.

modulate the activity of thrombin in the blood coagulation process.<sup>32–34</sup> The structures of these aptamer–thrombin complexes have been carefully characterized in solution previously, and they can serve as a good model system for the study of aptamer–protein and aptamer–protein–antibody structures on surfaces.

To successfully detect target proteins using the aptamer–protein–antibody sandwich structure, the aptamer and antibody must bind to different sites on the target protein. If the same binding site is involved, the aptamer–protein–antibody sandwich structure will not be created. This geometric requirement is illustrated schematically in Figure 2. Sequential SPRI measurements of thrombin and antibody adsorption onto RNA microarrays can determine which antibody–aptamer pairs will form surface sandwich structures.

A four-component microarray that consisted of three previously developed thrombin aptamers<sup>32–34</sup> and one control RNA aptamer sequence was fabricated for these SPRI experiments. A schematic diagram of the four aptamer sequences as well as the spatial pattern of the aptamer microarray is shown in Figure 3. The thrombin RNA aptamer  $R_1$  and thrombin DNA aptamer  $D_1$  were both developed with binding affinity to hTh.<sup>33,34</sup> In the  $D_1$  aptamer, the eight boxed guanine bases form a G-quadruplex that contributes to the binding of thrombin.<sup>34</sup> Thrombin RNA aptamer  $R_2$  was originally selected with affinity to bovine thrombin but can also bind to hTh.<sup>32</sup> The control sequence  $R_V$  is an RNA aptamer with binding affinity to VEGF that will be used in section C.

Two sequential in situ SPRI measurements on this microarray allowed us to identify which aptamer(s) can form the surface aptamer–hTh–antibody sandwich structure. The first SPRI measurement, shown in Figure 4a, was used to determine the amount of hTh adsorption onto the microarray from a 10 nM solution. All

three thrombin aptamers showed some binding affinity to hTh, with the  $D_1$  aptamer being the highest. A second SPRI measurement, shown in Figure 4b, was obtained after subsequent exposure of the array to a 10 nM solution of a monoclonal antibody for hTh. A significant SPRI signal increase was observed only at the  $R_2$  array elements, indicating that the antibody could only bind to the hTh– $R_2$  aptamer surface complex.

This set of experiments demonstrates that only the  $R_2$  aptamer binds to hTh at a different site as compared to the antibody. It is not surprising that  $R_2$ , an aptamer originally selected for bovine thrombin, can also bind to human thrombin since there is an 85% homology between the two proteins.<sup>32</sup> For the aptamer array elements that bind to the same site as the antibody, two results are possible: the hTh stays on the surface, and very little antibody adsorption is observed (as seen with the  $D_1$  elements), or the hTh is removed from the surface by the antibody (as seen with the  $R_1$  elements). No nonspecific adsorption of hTh or antibody binding was observed onto the control aptamer elements  $R_V$ .

These SPRI results agree with what is known of how these aptamers interact with hTh in solution. Human thrombin has an active catalytic site and two exosites; exosite I is implicated in the binding of fibrinogen, thrombomodulin, hirudin, and heparin cofactor II, and exosite II is primarily responsible for the binding to glycosaminoglycan, heparin, and monoclonal antibody.<sup>35–37</sup> Both aptamers  $D_1$  and  $R_1$  have been reported previously to bind to the heparin binding site–exosite II,<sup>33,34</sup> which is also the binding site to the monoclonal thrombin antibody.<sup>37</sup> This is consistent with our SPRI results that no antibody binding was observed for hTh molecules bound to either  $D_1$  or  $R_1$ . The  $R_2$  binding site on hTh has not been specifically reported previously, but from our SPRI measurements, we can conclude that  $R_2$  does not bind to exosite

(32) Liu, X.; Cao, G.; Ding, H.; Zhang, D.; Yang, G.; Liu, N.; Fan, M.; Shen, B.; Shao, N. *FEBS Lett.* **2004**, *562*, 125–128.  
 (33) White, R. R.; Rusconi, C. P.; Scardino, E.; Wolberg, A.; Lawson, J.; Hoffman, M.; Sullenger, B. A. *Mol. Ther.* **2001**, *4*, 567–573.  
 (34) Tasset, D. T.; Kubik, M. F.; Steiner, W. J. *Mol. Biol.* **1997**, *272*, 688–698.

(35) Di Cera, E. *Chest* **2003**, *124*, 11S–17S.  
 (36) Verhamme, I. M.; Olson, S. T.; Tollefsen, D. M.; Bock, P. E. *J. Biol. Chem.* **2002**, *277*, 6788–6798.  
 (37) Colwell, N. S.; Blinder, M. A.; Tsiang, M.; Gibbs, C. S.; Bock, P. E.; Tollefsen, D. M. *Biochemistry* **1998**, *37*, 15057–15065.

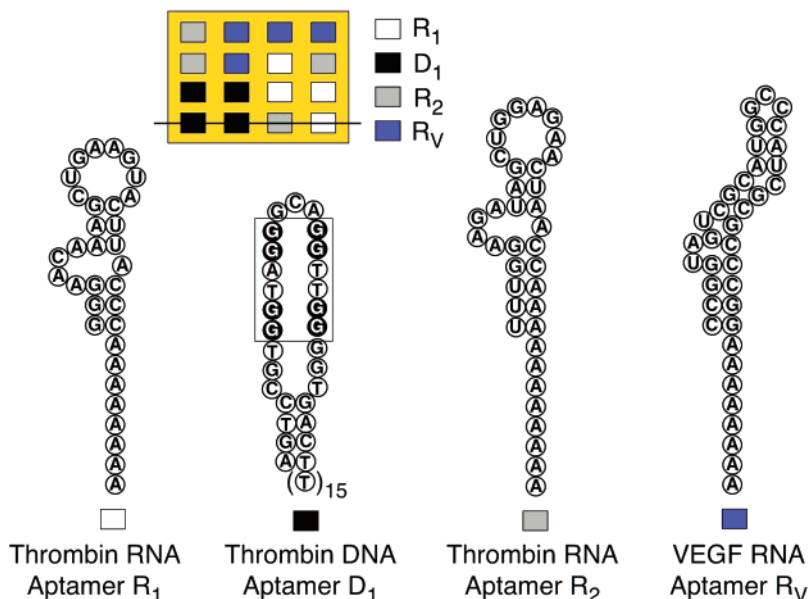


**Figure 3.** Structures of the aptamers used in a four-component microarray for the identification of a thrombin aptamer to be used for thrombin detection in a surface sandwich assay. The four aptamer array elements are:  $R_1$ , an RNA aptamer for human thrombin;  $D_1$ , a DNA aptamer for human thrombin;  $R_2$ , an RNA aptamer that was selected for bovine thrombin but can also bind to human thrombin;  $R_V$ , an RNA aptamer for human VEGF. The boxed guanine bases in the  $D_1$  aptamer form a G-quadruplex structure (not pictured) that is responsible for human thrombin binding.  $R_V$  was used as a negative control in the thrombin detection. The pattern of the four-component microarray is shown at the top of this figure.

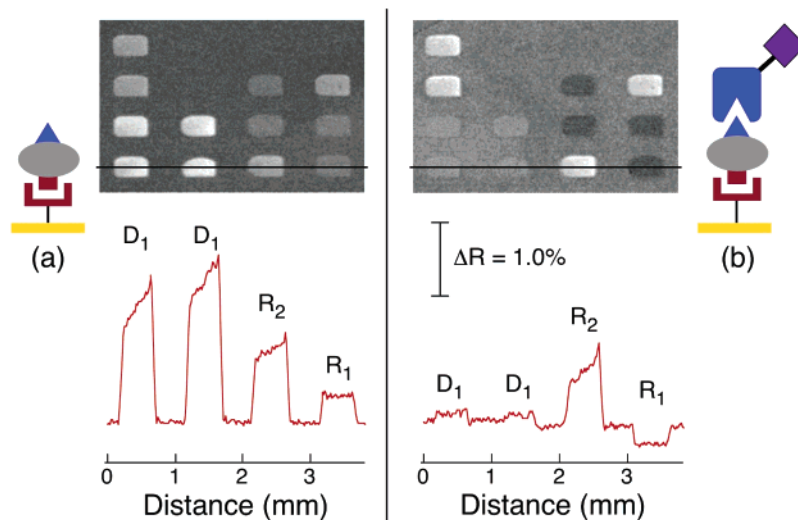


**Figure 4.** In situ SPRI measurements of the sequential binding of hTh and hTh antibody to a four-component microarray composed of  $R_1$ ,  $D_1$ ,  $R_2$ , and  $R_V$ . The pattern of the microarray is shown in Figure 3. (a) Surface adsorption of 10 nM hTh onto the microarray. The SPR difference image was obtained by subtracting images taken before and after the introduction of hTh. The line profile was taken from the last row on the difference image. All three of the thrombin aptamers,  $R_1$ ,  $R_2$ , and  $D_1$ , showed binding to hTh, but with different binding affinities.  $D_1$  has the highest affinity to thrombin, and  $R_1$  has the lowest. (b) Binding of 10 nM HRP-conjugated hTh antibody to the surface-bound hTh molecules. The SPR difference image was obtained by subtracting images acquired before and after the adsorption of hTh antibody with the corresponding line profile at the bottom taken across the last row of this difference image. No significant antibody binding was observed at the  $D_1$  array elements. The  $R_1$  aptamer array elements showed a decrease in signal due to the removal of surface-bound hTh molecules. Only  $R_2$  array elements exhibited significant antibody binding that suggests the formation of a surface aptamer–hTh–antibody sandwich structure.

II. Based on these results, we will exclusively use the  $R_2$  aptamer in the enzymatically amplified SPRI detection of hTh in the next section.

**B. Subpicomolar Thrombin Detection with Enzymatically Amplified SPRI.** Having identified the appropriate RNA aptamer to form the surface aptamer–protein–antibody structure, the surface precipitation reaction catalyzed by the enzyme HRP

was characterized with the detection of hTh at subpicomolar concentrations using enzymatically amplified SPRI. HRP has been used previously in conjunction with various detection techniques including fluorescence, SPR, and electrochemical methods for amplified detection of DNA and proteins.<sup>25,27,38</sup> This amplification reaction was necessary in order to lower the SPRI detection limit for hTh from nanomolar concentrations down to subpicomolar

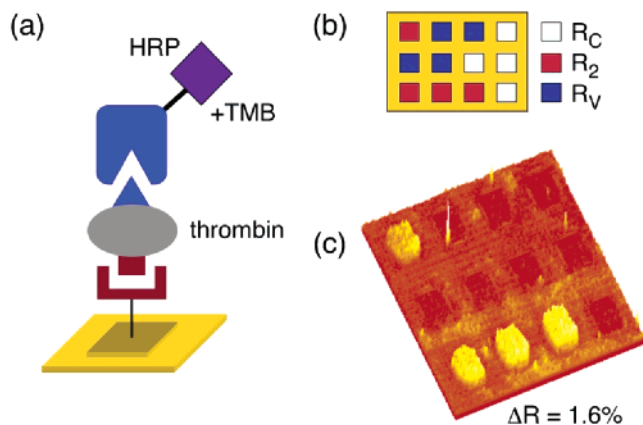


**Figure 5.** Enzymatically amplified SPRI detection of 500 fM hTh. (a) Schematic showing the surface  $R_2$  aptamer–hTh–HRP-conjugated antibody sandwich structure. This was created by sequentially flowing hTh and the HRP-conjugated monoclonal hTh antibody onto a surface-immobilized  $R_2$  aptamer. (b) Pattern of the three-component RNA microarray composed of  $R_2$ ,  $R_V$ , and  $R_C$  for hTh detection.  $R_2$  is the RNA aptamer for hTh,  $R_V$  is the RNA aptamer for VEGF, and  $R_C$  is a control RNA sequence with no hairpin structures (see Table 1 for sequences). (c) An SPR difference image obtained from the detection of 500 fM hTh using the HRP enzymatic amplification reaction. Only  $R_2$  aptamer array elements showed a 1.6% increase in  $\Delta R$ .

concentrations. An antibody conjugated with HRP was employed in the formation of the surface sandwich structure; Figure 5a shows schematically how the antibody–HRP conjugate formed a complex with hTh and the  $R_2$  aptamer on the array element surface.

The SPRI measurements employed a three-component microarray consisting of the thrombin aptamer  $R_2$ , the VEGF aptamer  $R_V$ , and a control RNA sequence  $R_C$  (see Figure 5b for the array pattern and Table 1 for all RNA sequences). The microarray was first exposed to a 500 fM hTh solution for 15 min, and then a 10 nM solution of the antibody–HRP conjugate for 10 min, followed by TMB for 10 min, and finally rinsed with buffer. The SPR difference image of this array before and after exposure to TMB is shown in Figure 5c. An SPRI reflectivity change ( $\Delta R$ ) of  $1.6 \pm 0.2\%$  was observed only on the  $R_2$  microarray elements due to the precipitation of TMB caused by the surface-bound HRP enzyme. Only an extremely small amount of precipitation was observed on the PEG array background, possibly due to nonspecific adsorption of the antibody–enzyme conjugate that has resulted in precipitation at these locations. Compared with the 2.0%  $\Delta R$  observed for a 10 nM hTh solution in Figure 4a, a 1.6%  $\Delta R$  for a 500 fM hTh solution corresponds to an enhancement factor of  $\sim 10^4$ . The SPRI signal from different array elements on the same microarray varied slightly with a standard deviation of less than 15%; the chip-to-chip variation of SPRI signal was found to be in a similar range.

The responsivity of this amplified SPRI method to thrombin adsorption was estimated with two additional SPRI measurements at thrombin concentrations of 1 ( $4.1 \pm 0.6\% \Delta R$ ) and 2 pM ( $8.7 \pm 1.3\% \Delta R$ ). The three data points (including our lowest concentration measurement at 0.5 pM) yielded a linear relationship between

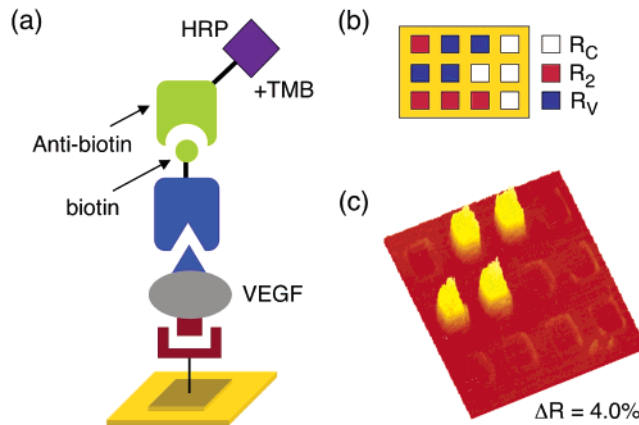


**Figure 6.** Enzymatically amplified SPRI detection of 1 pM VEGF. (a) Schematic illustrating the surface sandwich structure formed by the sequential adsorption of VEGF (1 pM), a biotinylated VEGF antibody (10 nM), and an anti-biotin-conjugated HRP (50 nM) onto VEGF aptamer array elements. (b) Pattern of the three-component RNA microarray consisting of  $R_2$ ,  $R_V$ , and  $R_C$  for VEGF detection. The RNA sequences are listed in Table 1. (c) An SPR difference image obtained from the detection of 1 pM VEGF with the HRP enzymatic amplification reaction. A  $\Delta R$  increase of  $\sim 4.0\%$  was observed at only the  $R_V$  array elements.

concentration and  $\Delta R$  with a slope of  $4.7 (\pm 0.1)\% \Delta R/\text{pM}$ . Above a  $\Delta R$  of 10%, this SPRI responsivity decreased as predicted by theory.<sup>17</sup> The protein concentration range over which the SPRI signal responds linearly can be optimized by adjusting the concentrations of both the hTh antibody–HRP conjugate and TMB substrate.

As mentioned previously, a little amount of nonlocalized precipitation was observed in Figure 5c. This additional precipitation is not due to the nonspecific adsorption of either protein or antibody onto the microarray, because no nonspecific adsorption onto the RNA microarray elements or the PEG background was observed in the SPRI experiments at higher nanomolar protein and antibody concentrations as shown in Figure 4a and b. A possible source for the nonlocalized precipitation is the desorption of antibody–HRP conjugates during the final rinse step and introduction of TMB. We attribute the lack of nonspecific adsorption of proteins or antibodies in these experiments to the use of RNA aptamer microarrays instead of antibody microarrays, where we have observed nonspecific protein interactions with antibodies previously.<sup>20</sup>

### C. Picomolar VEGF Detection with Enzymatically Amplified SPRI.

The surface HRP–TMB enzymatic precipitation reaction was next used for the amplified SPRI detection of the protein biomarker VEGF at a biologically relevant concentration. The concentration of VEGF is normally  $\sim 7$  pM in the serum; however, patients with certain diseases such as breast cancer and rheumatoid arthritis can have a considerably higher VEGF concentration.<sup>23,24</sup> A set of RNA aptamers for human VEGF that have all been shown to bind to the heparin binding site on the protein have been previously developed by Jellinek et al.<sup>39</sup> One of these aptamers has been successfully applied in an antibody sandwich assay for the detection of VEGF, implying that the anti-VEGF antibody does not bind to the heparin binding site.<sup>40</sup> We

(38) Kim, M.-G.; Shin, Y.-B.; Jung, J.-M.; Ro, H.-S.; Chung, B. H. *J. Immunol. Methods* **2005**, *297*, 125–132.

(39) Jellinek, D.; Green, L. S.; Bell, C.; Janjic, N. *Biochemistry* **1994**, *33*, 10450–10456.

therefore chose an RNA aptamer from the same set with a high binding affinity (denoted as  $R_V$ ; see Table 1 for the sequence) to use in the amplified SPRI measurements.

For the detection of VEGF with enzymatically amplified SPRI, we used a modified sandwich assay shown in Figure 6a. In this instance, a biotinylated VEGF antibody is employed to form the sandwich structure, and then an anti-biotin-conjugated HRP is used to attach the enzyme to this antibody. As in the previous thrombin experiments, the precipitation of TMB by HRP is used to detect the presence of VEGF on the microarray. The SPRI measurements employed a three-component RNA microarray composed of  $R_2$ ,  $R_V$ , and  $R_C$  (see Figure 6b for array pattern).

The VEGF detection sensitivity of the enzymatically amplified SPRI measurements is demonstrated in Figure 6c. The RNA microarray was first exposed to a 1 pM VEGF solution for 15 min, then a 10 nM solution of the VEGF antibody for 10 min, then the anti-biotin HRP solution (50 nM) for 10 min, and finally the TMB solution. The SPR difference image before and after exposure to TMB is shown in Figure 6c. An SPRI reflectivity change ( $\Delta R$ ) of +4.0% was observed at only the  $R_V$  array elements, indicating the presence of VEGF at these spots. Neither nonspecific adsorption nor extraneous precipitation was observed on the background or the noninteracting RNA array elements  $R_2$  and  $R_C$ .

The detection of a 1 pM solution of VEGF with enzymatically amplified SPRI is a great improvement over conventional SPRI measurements. Direct adsorption of VEGF onto surface-immobilized aptamers can only be detected with SPRI at concentrations higher than 10 nM. Detection of VEGF at picomolar concentrations is well below that needed for the analysis of VEGF from human plasma or serum samples.

(40) Drolet, D. W.; Moon-McDermott, L.; Romig, T. S. *Nat. Biotechnol.* **1996**, *14*, 1021–1025.

## CONCLUSIONS

In this paper, we have used a combination of RNA aptamers and antibodies to detect protein biomarkers at picomolar concentrations with HRP–TMB enzymatically amplified SPRI measurements of RNA aptamer microarrays. This sensitivity level is a 10 000-fold improvement over conventional SPRI measurements of protein adsorption onto RNA aptamer microarrays and is comparable to the sensitivity observed in fluorescence antibody sandwich assays.

Note that this detection method requires both an RNA aptamer and an antibody that binds to a different site on the target protein. However, since this antibody is not attached to the surface, issues of surface antibody activity and immobilization are avoided. Moreover, as additional RNA aptamers are discovered in the future, it should be possible to totally eliminate the antibody from this detection approach by replacement with a second biotinylated RNA aptamer. The development of new RNA aptamers with strong binding affinities will also allow for the creation of larger scale aptamer microarrays for the simultaneous analysis of multiple protein biomarkers.

## ACKNOWLEDGMENT

This research was supported by the National Institute of Health (2R01 GM059622-04) and the National Science Foundation (CHE-0551935).

Received for review October 2, 2006. Accepted November 13, 2006.

AC061849M